Synthesis and Structural Characterization of Two Tetraruthenium Bis(phosphinidene) Clusters with 62- and 64-Electron Counts: $Ru_4(CO)_{11}(\mu_4\text{-}PPh)(\mu_4\text{-}PNPr^i_2)$ and $Ru_4(CO)_{12}(\mu_4\text{-}PNPr^i_2)_2$

Weibin Wang,[†] John F. Corrigan,[‡] Gary D. Enright,[†] Nicholas J. Taylor,[‡] and Arthur J. Carty*[,†,§]

Steacie Institute for Molecular Sciences, National Research Council of Canada, 100 Sussex Drive, Ottawa, Ontario, Canada K1A 0R6, Department of Chemistry, University of Waterloo, Waterloo, Ontario, Canada N2L 3G1, and Ottawa-Carleton Chemistry Institute, Department of Chemistry, University of Ottawa, Ottawa, Ontario, Canada K1S 5B6

Received August 18, 1997

The clusters $Ru_4(CO)_{10}(\mu\text{-}CO)(\mu_4\text{-}PPh)(\mu_4\text{-}PNPr^i_2)$ (**6**) and $Ru_4(CO)_{12}(\mu_4\text{-}PNPr^i_2)_2$ (**7**) have been prepared via the reactions of $Cl_2PNPr^i_2$ with, respectively, $[Ru_4(CO)_{12})(\mu_3\text{-}PPh)]^{2-}$ (**5**) and $[Ru_4(CO)_{12}]^{4-}$. The dianion **5** has been generated from the reduction of $[Ru_4(CO)_{13})(\mu_3\text{-}PPh)]$ (**2**) by $CoCp_2$. The structures of $\mathbf{5}[CoCp_2]_2$, **6**, and **7** were determined by X-ray crystallography. The structure of the dianion **5** resembles that of its precursor $[Ru_4(CO)_{13})(\mu_3\text{-}PPh)]$ (**2**) and consists of a square pyramidal framework of four $Ru(CO)_3$ fragments with a PPh group occupying a basal position. Thus, loss of a CO ligand via two electron reduction leads to relatively small structural changes. There are 10 terminal carbonyls and 1 bridging carbonyl in **6**, and the four Ru atoms have a square planar arrangement with the two different phosphinidene ligands each capping one side of the Ru_4 square. There are, however, 12 terminal carbonyls in **7**, and the Ru_4 arrangement is a significantly puckered square (dihedral angle 135.4 °C). Each phosphinidene ligand in **7** caps one side of the Ru_4 framework and has two very long and two normal Ru−P distances. The P−P distance in **7** is 3.152 Å, the longest value reported to date for this type of M_4P_2 compound.

Introduction

Hoffmann, Saillard, and Halet[1] have examined in detail the electronic structure and bonding in clusters of the types $M_4(\mu_4\text{-}E)_2$, $M_4(\mu_4\text{-}E)$, and $M_4(\mu_3,\eta^2\text{-}E_2)$ (E = main-group element) in order to gain a better understanding of the various stable electron counts exhibited within these classes of molecules. Of particular interest in this series of compounds were the following observations:

(i) The prediction that compounds of the type $[Fe_4(CO)_{14}(\mu_4\text{-}PR)]$ (**1**), having a square pyramidal Fe_4P core with each Fe atom occupying a vertex of the square, should be accessible and stable. Clusters of this type would, thus, contain eight skeletal pairs and a total of 64 cluster valence electrons. To date however, the only related molecules which have been synthesized are of the type $M_4(CO)_{13}(\mu_3\text{-}PR)^2$ (**2**) (M = Ru, Os) which possess seven skeletal pairs and have *nido* structures with a μ_3-PR ligand occupying a basal site or $M_4(CO)_{12}(\mu_4\text{-}PR)$ (**3**) (M = Fe) which, with 60 electrons, have *closo* structures with an equatorial PR group.[3] Clusters of type **2** readily undergo skeletal isomerization in the presence of a four-electron donor (e.g., X = S, Se, Te) affording *trans* octahedral 62-electron $M_4(CO)_{11}(\mu_4\text{-}PR)(\mu_4\text{-}X)$ compounds.[4]

(ii) In clusters $M_4(CO)_{11}(\mu_4\text{-}PR)_2$ (**4**) (M = Fe, Ru), EHMO calculations provide evidence for "through the cluster" P···P bonding interactions.

(iii) The presence of a low-lying b_{1u} molecular orbital in clusters with $M_4(\mu_4\text{-}PR)_2$ cores (M = Fe, Ru) suggests that molecules with 62- (11 CO) or 64-electron (12 CO) counts should exist.

Our interest in the chemistry of the remarkable molecules $M_4(CO)_{13}(\mu_3\text{-}PR)$ **2** (M = Ru, Os) which serve as models for chemical transformations on square M_3P and M_4 faces[5] prompted us to explore whether the clusters **2** could be chemically reduced to 64-electron dianions $[M_4(CO)_{13}(\mu_{3\text{-}4}\text{-}PR)]^{2-}$ which might be structurally related to the $M_4(CO)_{14}(\mu_4\text{-}PR)$ compounds **1** predicted by Hoffmann et al. Such anions would also, via reaction with $R'PCl_2$, provide access to a new series of mixed-bis(phosphinidene) clusters $M_4(CO)_{11-12}(\mu_4\text{-}PR)(\mu_4\text{-}PR')$. In this paper, we describe the synthesis

[†] National Research Council of Canada.
[‡] University of Waterloo.
[§] University of Ottawa.

(1) (a) Halet, J.-F.; Hoffmann, R.; Saillard, J.-Y. *Inorg. Chem.* **1985**, *24*, 1695. (b) Halet, J.-F.; Saillard, J.-Y. *Nouv. J. Chim.* **1987**, *11*, 315.
(2) (a) Adams, R. D.; Belinski, J. A.; Pompeo, M. P. *Organometallics* **1992**, *11*, 3129. (b) Guldner, K.; Johnson, B. F. G.; Lewis, J. *J. Organomet. Chem.* **1988**, *355*, 419. (c) Adams, R. D.; Wang, S. *Inorg. Chem.* **1986**, *25*, 2534. (d) Süss-Fink, G.; Thewalt, U.; Klein, H.-P. *J. Organomet. Chem.* **1984**, *262*, 315. (e) Cherkas, A. A.; Corrigan, J. F.; Doherty, S.; MacLaughlin, S. A.; van Gastel, F.; Taylor, N. J.; Carty, A. J. *Inorg. Chem.* **1993**, *32*, 1662.
(3) Buchholz, D.; Huttner, G.; Imhof, W.; Orama, O. *J. Organomet. Chem.* **1990**, *388*, 321.
(4) (a) Corrigan, J. F.; Doherty, S.; Taylor, N. J.; Carty, A. J. *J. Chem. Soc., Chem. Commun.* **1991**, 1640. (b) Lunniss, J.; MacLaughlin, S. A.; Taylor, N. J.; Carty, A. J.; Sappa, E. *Organometallics* **1985**, *4*, 2066. (c) Adams, R. D.; Wang, S. *J. Am. Chem. Soc.* **1987**, *109*, 924.
(5) Sappa, E.; Tiripicchio, A.; Carty, A. J.; Toogood, G. E. *Prog. Inorg. Chem.* **1987**, *35*, 437.

S0276-7333(97)00726-7 CCC: $15.00
Publication on Web 01/13/1998

of $[Ru_4(CO)_{12}(\mu_3\text{-PPh})]^{2-}$ via reduction of **2** (M = Ru, R = Ph) with cobaltocene, the structural relationships between **2** and the dianion $[Ru_4(CO)_{12}(\mu_3\text{-PPh})]^{2-}$ (**5**), the synthesis of $Ru_4(CO)_{11}(\mu_4\text{-PPh})(\mu_4\text{-PNPr}^i_2)$ (**6**) and $Ru_4(CO)_{12}(\mu_4\text{-PNPr}^i_2)_2$ (**7**), and the differences in core Ru_4PP' frameworks in the 62- and 64-electron bis(phosphinidene) species.

Experimental Section

General Procedures. Syntheses were carried out using either a nitrogen-atmosphere glovebox or standard Schlenk techniques. Solvents, unless otherwise stated, were dried and distilled under nitrogen prior to use. Separation of products was accomplished by column chromatography and TLC using oven-dried (150 °C, over 48 h) silica gel (70−230 mesh). Infrared spectra were recorded on a Nicolet 520 FTIR spectrometer. NMR spectra were recorded on a Bruker AC-200 instrument at field strengths of 81.02 and 50.32 MHz, respectively, for $^{31}P\{^1H\}$ and $^{13}C\{^1H\}$ and on a Bruker AC-250 instrument at a field strength of 250 MHz for ^1H. Microanalyses were carried out by M-H-W Laboratories, Phoenix, AZ. All chemicals were commercially supplied and used without further purification. The compounds $Ru_4(CO)_{13}(\mu_3\text{-PPh})$[2e] and $Na_4[Ru_4(CO)_{12}]$[6] were prepared by the literature methods.

Preparation of $[Ru_4(CO)_{12}(\mu_3\text{-PPh})][CoCp_2]_2$ ($5[CoCp_2]_2$). To a solution of **2** (R = Ph) (396 mg, 0.452 mmol) in CH_2Cl_2 (10 mL) was added 2 equiv of $CoCp_2$ (171 mg, 0.905 mmol) in CH_2Cl_2 (2−3 mL) with vigorous stirring. A rapid reaction occurred, as evidenced by the precipitation of a purple microcrystalline solid and the evolution of CO gas. The solid was filtered through a fine-glass sintered frit and washed with CH_2Cl_2 to give a yield of 97% (540 mg) for $5[CoCp_2]_2$. Dark red single crystals obtained from cooling CH_3CN/CH_2Cl_2 solutions at −30 °C were used for microanalysis. IR (CH_3CN): ν(CO) 2023 w, 1981 s, 1950 vs cm^{-1}. ^1H NMR ($CDCl_3$): δ 7.62−7.53 (m, H_{phenyl}), 7.25−7.12 (m, H_{phenyl}), 5.62 (s, C_5H_5); $^{31}P\{^1H\}$ NMR (CD_3CN): δ 432 (s). $^{13}C\{^1H\}$ NMR (CD_3CN): δ 209.7 (d, *C*O, J_{PC} = 12.6 Hz), 161.5 (d, C_{ipso}, J_{PC} = 27.2 Hz), 131.6 (d, C_{ortho}, J_{PC} = 10.1 Hz), 127.7 (d, C_{meta}, J_{PC} = 8.0 Hz), 127.5 (s, C_{para}), 85.8 (s, C_5H_5). Anal. Calcd for $C_{38}H_{25}O_{12}PCo_2Ru_4$: C, 37.21; H, 2.05. Found: C, 35.66; H, 2.32.

Preparation of $Ru_4(CO)_{10}(\mu\text{-CO})(\mu_4\text{-PPh})(\mu_4\text{-PNPr}^i_2)$ (6). A sample of $5[CoCp_2]_2$ (115 mg, 93.8 mmol) was dissolved in 5 mL of CH_3CN, and 17 mL (118 mmol) of $Cl_2PNPr^i_2$ was added. An immediate color change from red to red/brown occurred with the addition of $AgBF_4$ (37 mg, 188 mmol). Monitoring the reaction via IR spectroscopy showed the disappearance of the starting material **5**. The solution was allowed to stir for 5 min, after which time the solvent was removed *in vacuo*. The residue was extracted into CH_2Cl_2 and separated via TLC (CH_2Cl_2/hexane, 20/80), yielding purple **6** (15 mg, 17%) as the only major product. IR (hexane): ν(CO) 2076 w, 2040 s, 2033 vs, 2017 s, 1981 m, 1833 w cm^{-1}. ^1H NMR ($CDCl_3$): δ 7.24−7.12 (m, H_{phenyl}, 3H), 6.73−6.61 (m, H_{ortho}, 2H), 2.77 (d sept, J_{PH} = 16.0 Hz, J_{HH} = 6.9 Hz, 2H), 0.84 (d, J_{HH} = 6.9 Hz, 12H). $^{31}P\{^1H\}$ NMR ($CDCl_3$): δ 249.6 (d, J_{PP} = 69 Hz, *P*NPr$^i_2$), 189.7 (d, J_{PP} = 69 Hz, *P*Ph). Anal. Calcd for $C_{23}H_{19}NO_{11}P_2Ru_4$: C, 29.02; H, 2.01. Found: C, 29.17; H, 2.06.

Preparation of $Ru_4(CO)_{12}(\mu_4\text{-PNPr}^i_2)_2$ (7). A mixture of $Ru_3(CO)_{12}$ (622 mg, 0.973 mmol), benzophenone (533 mg, 2.92 mmol) and potassium (114 mg, 2.92 mmol), was placed in a flask with a Teflon stopcock. To this mixture was added 12 mL of THF. The solution was then placed in an oil bath of 55−60 °C, stirred for 48 h, and cooled to room temperature followed by the dropwise addition of 210 μL (1.42 mmol) of $Cl_2PNPr^i_2$. Removal of the solvent and column chromatography of the residue with hexane as the eluant led to isolation of the desired product. Air-stable, dark red crystals of **7** (117 mg, 16%) were obtained from the recrystallization from CH_2Cl_2/MeOH at −10 °C. IR (CH_2Cl_2): ν(CO) 2054 w, 2040 s, 2000 m, 1969 w cm^{-1}. ^1H NMR ($CDCl_3$): δ 5.52 (sept, J_{HH} = 7.1 Hz, CH), 1.61 (d, J_{HH} = 7.1 Hz, CH_3). $^{31}P\{^1H\}$ NMR ($CDCl_3$): δ 444.8(br, s). Anal. Calcd for $C_{24}H_{28}N_2O_{12}P_2Ru_4$: C, 28.75; H, 2.79. Found: C, 28.84; H, 3.00.

X-ray Analyses. Single crystals of each compound were obtained from recrystallization as follows: from CH_3CN/CH_2Cl_2 at room temperature for $5[CoCp_2]_2$; the slow evaporation of CH_2Cl_2/hexane solutions at room temperature for **6**; and CH_2Cl_2/CH_3OH at −10 °C for **7**. The intensity data of $5[CoCp_2]_2$ and **6** were collected on an LT-2-equipped Siemens R3m/V diffractometer with the use of graphite-monochromated Mo Kα radiation, while the intensity data of **7** were collected on an Enraf-Nonius CAD-4F diffractometer with the use of graphite-monochromated Cu Kα radiation. Background measurements were made by extending the scan width by 25% on each side of the scan for $5[CoCp_2]_2$ and **6** or by taking a stationary background count at each end of the scan (for 1/10 the scan time) combined with the profile analysis[7] for **7**. Absorption corrections were applied to the intensity data using the face-indexed numerical method.

The positions of the metal atoms were determined by Patterson syntheses for $5[CoCp_2]_2$ and direct methods for **6** and **7**. Subsequent electron density difference maps revealed the remaining non-hydrogen atoms. The two independent molecules in the asymmetric unit cell of **6** are structurally very similar, although the isopropyl substituents on the nitrogen atom of molecule 2 were found to be highly disordered. A satisfactory model with 2-fold disorder and one-half a further 2-fold disorder for the two carbon atoms bonded to nitrogen was obtained with occupancies of 50:50:50:25:25 over five resolved sites. The molecule of compound **7** sits on a special (2-fold) position. All non-hydrogen atoms were refined anisotropically except the partially occupied sites of carbon atoms in **6**. Hydrogen atoms were included in calculated positions with refined isotropic thermal parameters for $5[CoCp_2]_2$ and fixed isotropic thermal parameters for **6** and **7**. Complex scattering factors[8] for neutral atoms were used in the calculation of the structure factors. All computations were carried out on Micro Vax II and Vax 3000 computers and Silicon Graphics Indigo work stations using SHELXTL software and the NRCVAX[7a] crystal structure system. Crystallographic data are summarized in Table 1. Selected bond lengths and angles for $5[CoCp_2]_2$, **6**, and **7** are tabulated in Tables 2, 3, and 4, respectively.

Results and Discussion

$[Ru_4(CO)_{12}(\mu_3\text{-PPh})]^{2-}$ (5). The reduction of $Ru_4(CO)_{13}(\mu_3\text{-PPh})$ (**2**) by 2 equiv of cobaltocene, $CoCp_2$, led to an immediate color change from red to deep purple within a few seconds and the formation of a purple precipitate ($5[CoCp_2]_2$) accompanied by a vigorous evolution of CO gas (eq 1). Complex $5[CoCp_2]_2$ is insoluble

$$\underset{\mathbf{2}}{Ru_4(CO)_{13}(\mu_3\text{-PPh})} + 2CoCp_2 \xrightarrow{-CO} \underset{\mathbf{5}[CoCp_2]_2}{[Ru_4(CO)_{12}(\mu_3\text{-PPh})]\,[CoCp_2]_2} \quad (1)$$

(6) Bhattacharyya, A. A.; Nagel, C. C.; Shore, S. G. *Organometallics* **1983**, *2*, 1187.

(7) (a) Gabe, E. J.; LePage, Y.; Charland, J.-P.; Lee, F. L.; White, P. S. *J. Appl. Crystallogr.* **1989**, *22*, 384. (b) Grant, D. F.; Gabe, E. J. *J. Appl. Crystallogr.* **1978**, *11*, 114.

(8) (a) *International Tables for X-ray Crystallography*; Kynoch Press: Birmingham, England, 1974; Vol. IV, p 99. (b) Stewart, R. F.; Davidson, E. R.; Simpson, W. T. *J. Chem. Phys.* **1965**, *42*, 3175.

Table 1. Summary of Crystal Data and Details of Intensity Collection for 5[CoCp$_2$]$_2$, 6, and 7

compound	**5**[CoCp$_2$]$_2$	**6**	**7**
mol formula	$C_{38}H_{25}O_{12}PCo_2Ru_4$	$C_{23}H_{19}NO_{11}P_2Ru_4$	$C_{24}H_{28}N_2O_{12}P_2Ru_4$
fw	1226.7	951.6	1002.71
temp (K)	180	295	295
cryst syst	monoclinic	triclinic	tetragonal
space group	$P2_1/n$	$P\bar{1}$	$P\bar{4}2d$
a, Å	14.805(2)	11.302(1)	24.276(1)
b, Å	13.216(2)	15.851(2)	
c, Å	20.570(4)	18.556(2)	12.094(1)
α, deg		102.70(1)	
β, deg	102.00(2)	107.26(1)	
γ, deg		91.12(1)	
V, Å^3	3936.9(11)	3084.0(6)	7127.7(5)
Z	4	4	8
D_{calc}, g cm^{-3}	2.070	2.050	1.869
μ(Mo Kα), cm^{-1}	24.21	20.80	151.8[a]
cryst size, mm	0.10 × 0.69 × 0.44	0.18 × 0.19 × 0.035	0.090 × 0.24 × 0.34
transmission coeff range[b]	0.373−0.789	0.658−0.881	0.0827−0.361
scan method	ω	ω	ω−2θ
scan width (ω), deg	1.50	1.20	1.0 + 0.15 tan θ
scan rate (ω), deg min^{-1}	2.93−29.30	2.93−29.30	2
scan range (2θ), deg	4−52	4−48	4−140
no. of unique rflns	7790	9728	3399
no. of obsd rflns[c]	6201	5877	3174
no. of variables	540	697	200
R[d]	0.026	0.030	0.032
R_w[e]	0.028	0.033	0.041
GOF[f]	2.04	1.71	1.61

[a] Cu Kα radiation was used. [b] Absorption corrections. [c] $F_o > 6\sigma(F_o)$ for **5**[CoCp$_2$]$_2$ and **6**, and $I_o > 2.5\sigma(I_o)$ for **7**. [d] $R = \sum||F_o| - |F_c||/\sum|F_o|$. [e] $R_w = (\sum w(|F_o| - |F_c|)^2/\sum w|F_o|^2)^{1/2}$, $w = [\sigma^2(F_o)]^{-1}$ for **5**[CoCp$_2$]$_2$ and **6**, and $w = [\sigma^2(F_o) + 0.0004(F_o)^2]^{-1}$ for **7**. [f] GOF = $(\sum w(|F_o| - |F_c|)^2/$(degrees of freedom))$^{1/2}$.

Table 2. Selected Bond Lengths (Å) for 5

Ru(1)−Ru(2)	2.915(1)	Ru(1)−Ru(3)	2.852(1)
Ru(2)−Ru(3)	2.790(1)	Ru(2)−Ru(4)	2.897(1)
Ru(3)−Ru(4)	2.863(1)	Ru(1)−P(1)	2.294(1)
Ru(2)−P(1)	2.344(1)	Ru(4)−P(1)	2.289(1)
P(1)−C(1)	1.841(4)		

Table 3. Selected Bond Lengths (Å) for 6

Ru(11)−Ru(21)	2.724(1)	Ru(11)−Ru(41)	2.869(1)
Ru(21)−Ru(31)	2.892(1)	Ru(31)−Ru(41)	2.869(1)
Ru(11)−P(11)	2.469(2)	Ru(11)−P(21)	2.542(2)
Ru(21)−P(11)	2.447(2)	Ru(21)−P(21)	2.517(3)
Ru(31)−P(11)	2.389(2)	Ru(31)−P(21)	2.412(2)
Ru(41)−P(11)	2.380(2)	Ru(41)−P(21)	2.441(2)
P(11)−C(121)	1.812(7)	P(21)−N(11)	1.668(7)

Table 4. Selected Bond Lengths (Å) for 7

Ru(1)−Ru(1a)	2.853(1)	Ru(1)−Ru(2a)	2.873(1)
Ru(2)−Ru(2a)	2.872(1)	Ru(1)−P(1)	2.273(2)
Ru(1)−P(1a)	2.812(2)	Ru(2)−P(1)	2.278(2)
Ru(2)−P(1a)	2.737(2)	P(1)···P(1a)	3.152(4)

in all common halogenated and aromatic solvents. It is extremely sensitive to traces of oxygen and gradually decomposes on standing in solution (CH_3CN). Carrying out the experiment under an atmosphere of CO gas (purge) did not circumvent the expulsion of CO from **2** and the formation of **5**.

The infrared spectrum of **5**[CoCp$_2$]$_2$ showed, by comparison with that of **2**, a dramatic shift to lower frequency of the ν(CO) stretching frequencies, consistent with greater back-donation into the π^* CO molecular orbitals due to the increased electron density on the metal atoms due to the doubly negative charge and the presence of one less CO group than in **2**. The solution spectrum also suggested the absence of μ-CO ligands. ^{1}H and ^{13}C{^{1}H} NMR spectra of **5**[CoCp$_2$]$_2$ confirmed the presence of both a PPh unit and Cp ligands. The carbonyl ligands were all in rapid exchange at room temperature, with only a single resonance being observed in the expected downfield region (δ = 209.7 ppm, J_{PC} = 12.6 Hz). The ^{31}P{^{1}H} NMR spectrum indicated little change from that of the starting material in the chemical shift observed for the phosphinidene ligand (δ = 432 ppm; cf. δ = 409 ppm for **2**), and this, in conjunction with the observed evolution of CO gas, suggested that the cluster had not undergone structural rearrangement but had instead been subjected to a two-electron reduction with the concomitant expulsion of a carbonyl ligand to form the 62-electron anionic species **5**.

A single-crystal X-ray analysis was carried out to determine the precise structural features of **5**. Satisfactory solution and refinement of the data confirmed the identity of the reduced species as [Ru$_4$(CO)$_{12}$(μ_3-PPh)][CoCp$_2$]$_2$ (**5**[CoCp$_2$]$_2$). The molecular structure of **5** is shown in Figure 1. The crystal structure consists of discrete anions [Ru$_4$(CO)$_{12}$(μ_3-PPh)]$^{2-}$ packed in the lattice with two cobalticenium cations. An interesting feature of the cations is that one [(η^5-C$_5$H$_5$)$_2$Co]$^+$ has eclipsed C$_5$H$_5$ rings while in the other the rings are staggered. The *nido* square pyramidal M$_4$P stereochemistry has been retained on going from neutral **2** to anionic **5** with the phosphorus atom still occupying a vertex of the base of the pyramid in **5**. However, each ruthenium atom in **5** is now coordinated to only three terminal carbonyls. A comparison of the structures of **2** and **5** confirms that the Ru(CO)$_4$ group of **2** has lost a carbonyl on two-electron reduction. The exact CO ligand eliminated is unknown and, indeed, given the dynamics of **2** at ambient temperatures,[2e] would be very difficult to determine.[9] However, it is worth noting that ligand substitution reactions of **2** invariably occur at the hinge atom Ru(3), as for example in [Ru$_4$(CO)$_{12}$(μ_3-PPh)-

(9) Darensbourg, D. J. in *The Chemistry of Metal Cluster Complexes*; Shriver, D. F., Kaesz, H. D., Adams, R. D., Eds.; VCH: New York, 1990.

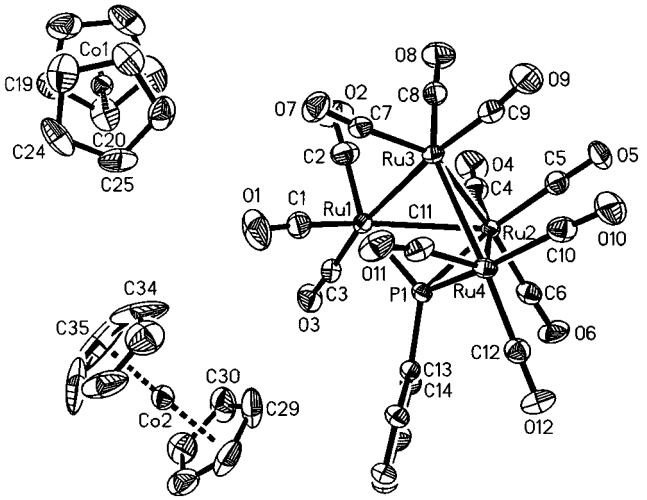

Figure 1. Molecular structure of $[Ru_4(CO)_{12}(\mu_3\text{-PPh})][Cp_2Co]$ (**5**$[Cp_2Co]$).

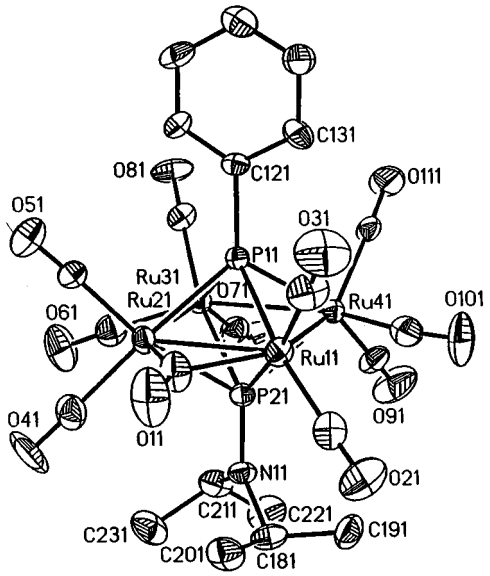

Figure 2. Molecular structure of $Ru_4(CO)_{10}(\mu\text{-CO})(\mu_4\text{-PPh})(\mu_4\text{-PNPr}^i_2)$ (**6**). Only molecule 1 of the two molecules in the asymmetric unit is shown.

$(PhPMe_2)]$[10] and $[Ru_4(CO)_{10}(\mu_3\text{-PPh})(\eta^6\text{-}C_7H_8)]$,[10] whose structures have been established by X-ray diffraction. Unlike the two-electron reduction of polynuclear carbonyls (e.g., $Os_3(CO)_{12} \rightarrow [Os_3(CO)_{10}(\mu\text{-CO})]^{2-}$)[11] which frequently results in the creation of bridging CO ligands (see also $[Ru_4(CO)_{12}(\mu_4\text{-PhC}{\equiv}\text{CPh})]$[12] and $[Et_4N]_2[Ru_4(CO)_9(\mu\text{-CO})_2(\mu_4\text{-PhC}{\equiv}\text{CPh})]$),[13] the conversion of **2** to **5** leaves all CO groups in the dianion **5** in terminal sites.

The average Ru−Ru bond length (Table 2) of **5** (2.863 Å) is identical within experimental error to that of **2** (2.867 Å). There is, however, a marked change in the pattern of the shorter/longer Ru−Ru distances. The shortest M−M distance in **5** is the one between the two hinge metal atoms Ru(2) and R(3) (2.790(1) Å) while this is the longest M−M bond in **2** (2.941(1) Å). One striking and contrasting feature between the two related clusters is the substantial contraction of all three of the ruthenium−phosphorus contacts on going from **2** (2.328(2) Å average) to **5** (2.309(2) Å average). One possible explanation for this contraction is that ruthenium−phosphorus back-bonding is increased in **5** to compensate for the negative charge on the Ru_4 core and the loss of a CO group.

Unsymmetrically Capped Bis(phosphinidene) Cluster $Ru_4(CO)_{10}(\mu\text{-CO})(\mu_4\text{-PPh})(\mu_4\text{-PNPr}^i_2)$] (6). The reaction of **5**$[CoCp_2]_2$ with 1 equiv of $Cl_2PNPr^i_2$ in the presence of $AgBF_4$ led to the rapid formation of cluster $[Ru_4(CO)_{10}(\mu\text{-CO})(\mu_4\text{-PPh})(\mu_4\text{-PNPr}^i_2)]$ (**6**), as shown in eq 2. In the absence of $AgBF_4$, however, no

$$\underset{\mathbf{5}}{[Ru_4(CO)_{12}(\mu_3\text{-PPh})]^{2-}} + Cl_2PNPr^i_2 \xrightarrow[-CO]{AgBF_4} \underset{\mathbf{6}}{[Ru_4(CO)_{11}(\mu_4\text{-PPh})(\mu_4\text{-PNPr}^i_2)]} \quad (2)$$

reaction was observed. Prolonged reaction times did not result in any increase in the recovered yield of **6** but led to the precipitation of an orange solid material which was completely insoluble in all common solvents. Its identity was not further investigated.

The IR spectrum of **6** shows a weak band at 1833 w cm^{-1}, suggesting the existence of a bridging carbonyl ligand. The $^{31}P\{^1H\}$ spectrum of **6** displays two signals, δ 249.6 (d, $J_{PP} = 69$ Hz, μ_4-*P*NPr^i_2) and 189.7 (d, $J_{PP} = 69$ Hz, μ_4-*P*Ph), at relatively high field compared to μ_4-PR ligands capping electron-precise M_4 clusters[14] and characteristic of "electron deficient" 62-electron square planar metal complexes.[15] High-field shifts are also observed in the ^1H NMR spectrum of **6** for the signals assigned to the *ortho* protons on the phenyl ring (6.66 ppm). Complexes of this type are highly fluxional, with only one CO resonance observed in the ^{13}C NMR spectrum at room temperature and no noticeable broadening of the signal upon cooling to the lowest accessible temperatures.[15] Even more remarkable is the fact that the carbonyl ligands on the polysubstituted derivatives of the general formula $[Fe_4(\mu_4\text{-PR})_2\{P(OMe)_3\}_x(CO)_y]$ ($x = 1-4$, $y = 11-7$) also undergo facile exchange, the replacement of CO by $P(OMe)_3$ having a negligible effect on the ligand-scrambling process.

A single-crystal X-ray analysis confirmed the proposed formula of **6** (Figure 2). Cluster **6** crystallizes with two crystallographically inequivalent but structurally similar molecules in the asymmetric unit, and all bond lengths and angles (Table 3) refer to molecule 1. To our knowledge, this is the first unsymmetrical bis(phosphinidene) complex of this type to be synthesized.

(10) van Gastel, F. Ph.D. Dissertation, University of Waterloo, 1991.
(11) (a) Krause, J. A.; Siriwardane, U.; Salupo, T. A.; Werner, J. R.; Knoeppel, D. W.; Shore, S. G. *J. Organomet. Chem.* **1993**, *454*, 263. (b) Churchill, M. R.; DeBoer, B. G. *Inorg. Chem.* **1977**, *16*, 878.
(12) (a) Johnson, B. F. G.; Lewis, J.; Schorpp, K. T. *J. Organomet. Chem.* **1975**, *91*, C13. (b) Johnson, B. F. G.; Lewis, J.; Reichert, B. E.; Schorpp, K. T.; Sheldrick, G. M. *J. Chem. Soc., Dalton Trans.* **1977**, 1417. (c) Jackson, P. F.; Johnson, B. F. G.; Lewis, J.; Raithby, P. R.; Will, G. J.; McPartlin, M.; Nelson, W. J. H. *J. Chem. Soc., Chem. Commun.* **1980**, 1190.
(13) Wang, J.; Sabat, M.; Lyons, L. J.; Shriver, D. F. *Inorg. Chem.* **1991**, *30*, 382.
(14) Carty, A. J.; MacLaughlin, S. A.; Nucciarone, D. In *Phosphorus-31 NMR Spectroscopy in Stereochemical Analysis: Organic Compounds and Metal Complexes*; Verkade, J. G., Quinn, L. D., Eds; VCH: New York, 1987; Chapter 16.
(15) (a) Jaeger, T.; Aime, S.; Vahrenkamp, H. *Organometallics* **1986**, *5*, 245. (b) Field, J. S.; Haines, R. J.; Smit, D. N. *J. Chem. Soc., Dalton Trans.* **1988**, 1315.

Indeed, the synthetic route to **6** should, in principle, be applicable to a wide range of mixed-phosphinidene complexes. The metal core consists of a near planar array of ruthenium atoms comprising three normal bond lengths and one significantly shortened Ru(11)−Ru(21) bond length, the latter vector being symmetrically bridged by a carbonyl ligand. These distances parallel those previously reported for the related symmetrical cluster $[Ru_4(CO)_{10}(\mu\text{-CO})(\mu_4\text{-PPh})_2]$.[16] There is also a semibridging CO ligand bonded to Ru(41) and tilted toward Ru(11) (Ru(41)−C(101)−O(101) = 162.8(11)°). The two phosphinidene ligands cap opposite sides of the M_4 plane with the average Ru−$PNPr^i_2$ distance (2.478 Å) significantly elongated compared to that observed for the Ru−PPh interactions (2.421 Å). Whether this reflects a better π-acceptor capability for PPh *vs* $PNPr^i_2$ or greater steric repulsion between the metal-ligand envelope and the $PNPr^i_2$ ligand is uncertain. These distances are both significantly longer, however, than the Ru−P bond lengths observed for **2** (2.332(1) Å) and $Ru_4(CO)_{13}(\mu_3\text{-}PNPr^i_2)$[17] (2.348(1) Å).

The ground-state structures of these clusters, as determined by diffraction methods (see references in ref 1), are characterized by the presence of at least one μ_2-CO ligand spanning a short metal−metal contact. Frequently, semibridging carbonyl groups are also present about the M_4 plane. These $M_4(CO)_{11-12}(\mu_4\text{-PR})_2$ (M = Fe, Ru) clusters pose an interesting challenge for localized (18-electron or EAN rules) and delocalized polyhedral skeletal electron pair (PSEP) bonding models.[18] Within the formalism of the 18-electron rule, the 62-electron square $M_4(CO)_{11}(\mu_4\text{-PR})_2$ clusters are electronically unsaturated, and a formal double bond has been proposed between the two 17-electron centers bridged by the μ-CO group. Concomitant movement of the double bond around the Ru_4 ring and carbonyl migration could provide a mechanism for some degree of delocalization within the unsaturated M_4 fragment.[15a] On the other hand, the PSEP approach provides a more satisfying description for $M_4(CO)_{11}(\mu_4\text{-PR})_2$, since with seven skeletal electron pairs and four metal atoms, an *arachno* $n + 3$ pair M_4 framework (or alternatively a *closo* $n + 1$ pair M_4P_2 skeleton) is predicted, as observed.

There is a further contrast in bonding model descriptions for $M_4(CO)_{12}(\mu_4\text{-PR})_2$. The iron clusters $Fe_4(CO)_{10}(\mu\text{-CO})(\mu_4\text{-PR})_2$ readily add nucleophiles, generating the 64-electron species $Fe_4(CO)_{11}(L)(\mu_4\text{-PR})_2$ (L = CO, LNR, PR_3).[15,19] From the EAN rule perspective, the latter clusters are electron-precise (4 Fe−Fe) with no short metal−metal bonds. However, structural distortions accompany nucleophilic addition. Thus, while the 62-electron $Fe_4(CO)_{11}(\mu_4\text{-PR})_2$ clusters have square planar Fe_4 frameworks, the corresponding 64-electron $Fe_4(CO)_{11}(L)(\mu_4\text{-PR})_2$ compounds possess a puckered Fe_4 core with disparate Fe−P contacts.[15a,19,20] The PSEP approach does not give a good fit with the structures of these molecules, since with eight skeletal electron pairs, the metal framework should be *hypho* ($n + 4$ pairs) or *nido* ($n + 2$) for a six vertex Fe_4P_2 skeleton.

The inadequacy of any simple electron counting model to explain all of the structural features of $M_4(CO)_{11-12}(\mu\text{-PR})_2$ clusters may indicate that these M_4P_2 systems lie in the transition region between localized and delocalized bonding.

The synthetic routes first employed to access these unsaturated clusters involved pyrolysis of a binary metal carbonyl in the presence of primary phosphines affording the desired complexes in low yield.[15b,16] Subsequent reports by Vahrenkamp and co-workers detailed a more rational pathway involving condensation reactions between either $Fe_3(CO)_{12}$ or $Ru_3(CO)_{12}$ and the dimer $[Fe_2(CO)_6(\mu\text{-PRH})_2]$ to yield the corresponding homo- and heterometallic complexes.[20,21] There are no reports describing the synthesis of unsymmetrically capped M_4PP' clusters, although mixed group 15/16 bicapped Ru_4 and Fe_4 clusters have been structurally characterized.[22] There are also reports on related bis(sulfido) and -(selenido) clusters,[23,24] mixed-metal-mixed-chalcogenide (Fe/Ru/Se/Te) M_4E_2 complexes,[24] and congeners containing heavier group V elements.[25]

$Ru_4(CO)_{12}(\mu_4\text{-}PNPr^i_2)_2$ (7). Complex **7** was formed by the addition of $Cl_2PNPr^i_2$ to a solution of $\{[Ru_4(CO)_{12}]^{4-}\}$[6] in THF and isolated after chromatography and recrystallization as a red solid (eq 3). This synthetic

$$[Ru_4(CO)_{12}]^{4-} + 2Cl_2PNPr^i_2 \rightarrow \underset{\mathbf{7}}{Ru_4(CO)_{12}(\mu_4\text{-}PNPr^i_2)_2} \quad (3)$$

route gives relatively low yields but is simple and convenient.

The structure (Figure 3) of **7** reveals an Ru_4P_2 arrangement with the two phosphinidene ligands each capping one side of the Ru_4 square, similar to **6** and other M_4E_2 types of compounds. The Ru_4 square, however, is severely puckered with a dihedral angle between the two Ru_3 planes of 135.4°. This is significantly smaller than that of $Fe_4(CO)_{11}[P(OMe)_3](P\text{-}p\text{-Tol})_2$ (163°),[19] so the degree of distortion from a square is much greater for the Ru_4 cluster. The molecule has a

(16) Field, J. S.; Haines, R. J.; Smit, D. N. *J. Organomet. Chem.* **1982**, *224*, C49.
(17) (a) Corrigan, J. F.; Doherty, S.; Taylor, N. J.; Carty A. J. *J. Am. Chem. Soc.* **1994**, *116*, 9799. (b) Wang, W.; Corrigan, J. F.; Doherty, S.; Enright, G. D.; Taylor, N. J.; Carty A. J. *Organometallics* **1996**, *15*, 2770.
(18) (a) Wade, K. *Adv. Inorg. Chem. Radiochem.* **1976**, *18*, 1. (b) Williams, R. E. *Adv. Inorg. Chem. Radiochem.* **1976**, *18*, 67. (c) Rudolph, R. W. *Acc. Chem. Res.* **1976**, *9*, 446. (d) Mingos, D. M. P. *Acc. Chem. Res.* **1984**, *17*, 311. (e) Mingos, D. M. P.; Wales, D. J. *Introduction to Cluster Chemistry*; Prentice Hall: Englewood Cliffs, 1990.
(19) Vahrenkamp, H.; Wolters, D. *Organometallics* **1982**, *1*, 874.
(20) (a) Vahrenkamp, H.; Wolters, D. *J. Organomet. Chem.* **1982**, *224*, C17. (b) Vahrenkamp, H.; Wucherer, E. J.; Wolters, D. *Chem. Ber.* **1983**, *116*, 1219.
(21) Jaeger, J. T.; Vahrenkamp, H. *Organometallics* **1988**, *7*, 1746.
(22) (a) van Gastel, F.; Agocs, L.; Cherkas, A. A.; Corrigan, J. F.; Doherty, S.; Ramachandran, R.; Taylor, N. J.; Carty, A. J. *J. Cluster Sci.* **1991**, *2*, 131. (b) Eber, D.; Buchholz, D.; Huttner, G.; Fässler, Th.; Imhof, W.; Fritz, M.; Jochims, J.; Daran, J. C.; Jeannin, Y. *J. Organomet. Chem.* **1991**, *401*, 49.
(23) (a) Adams, R. D.; Wolfe, T. A.; Wu, W. *Polyhedron* **1991**, *10*, 447. (b) Adams, R. D.; Babin, J. E.; Wang, J.-G. *Polyhedron* **1989**, *8*, 2351. (c) Adams, R. D.; Babin, J. E.; Tasi, M. *Inorg. Chem.* **1986**, *25*, 4514.
(24) (a) Mathur, P.; Hossain, Md. M.; Rashid, R. S. *J. Organomet. Chem.* **1994**, *467*, 245. (b) Mathur, P.; Hossain, Md. M.; Rashid, R. S. *J. Organomet. Chem.* **1993**, *460*, 83. (c) Layer, T. M.; Lewis, J.; Martin, A.; Raithby, P. R.; Wong, W.-T. *J. Chem. Soc., Dalton Trans.* **1992**, 3411. (d) Mathur, P.; Chakrabarky, D.; Hossain, Md. M. *J. Organomet. Chem.* **1991**, *418*, 415. (e) Mathur, P.; Thimmappa, B. H. S.; Rheingold, A. L. *Inorg. Chem.* **1990**, *29*, 4658.
(25) (a) Ang, H. G.; Hay, C. M.; Johnson, B. F. G.; Lewis, J.; Raithby, P. R.; Whitton, A. J. *J. Organomet. Chem.* **1987**, *330*, C7. (b) Hay, C. M.; Johnson, B. F. G.; Lewis, J.; Raithby, P. R.; Whitton, A. J. *J. Chem. Soc., Dalton Trans.* **1988**, 2091.

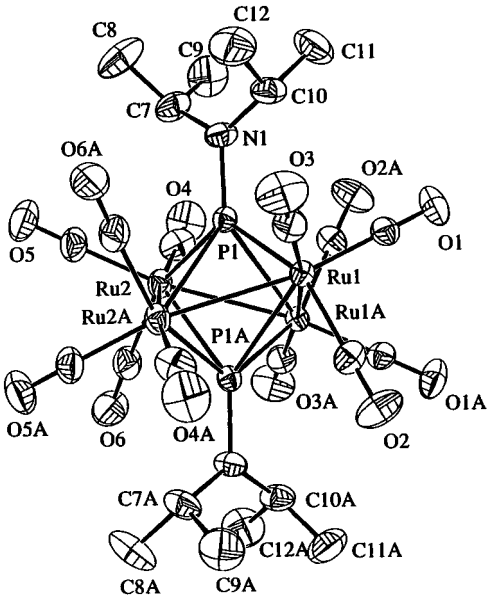

Figure 3. Molecular structure of $Ru_4(CO)_{12}(\mu_4\text{-}PNPr^i_2)_2$ (**7**).

crystallographic 2-fold symmetry with the axis passing through the midpoint of each of the Ru(1)−Ru(1a) and Ru(2)−Ru(2a) bonds. The M−M bond lengths (Table 4) in **7** are virtually equivalent with a variation of only 0.02 Å. The M−P distances, however, are very different. There are two normal M−P bond lengths (2.273(2) and 2.278(2) Å) and two very long M−P distances (2.812(2) and 2.737(2) Å) for each phosphorus atom. In other words, the phosphinidene ligands can almost be considered as μ_2-ligands, each bridging two nonadjacent ruthenium atoms of the Ru_4 square. Another significant feature in **7** is the P−P distance. While the P−P distance in the iron cluster $Fe_4(CO)_{11}[P(OMe)_3](P\text{-}p\text{-}Tol)_2$ is 2.598 Å, it is 3.152 Å in **7**, the longest value reported for these M_4P_2 compounds. At this distance, the presence of a "through the cluster" P···P interaction of the type described by Hoffmann, Saillard, and Halet is much reduced.

Cluster **7** contains 12 terminal carbonyl ligands, therefore, it has eight skeletal electron pairs. It is interesting, therefore, that addition of carbon monoxide to $Ru_4(CO)_{11}(PPh)_2$ does not lead to $Ru_4(CO)_{12}(PPh)_2$ but instead proceeds via M−M bond cleavage and the generation of $Ru_4(CO)_{13}(PPh)_2$. This is in direct contrast with the corresponding reaction of its Fe analogue.[26] The electronic structure of the model $M_4(CO)_{12}(\mu_4\text{-}PH)_2$ compounds has been studied in detail.[1] Extended Hückel calculations suggest that when M = Ru, the eight skeletal pair (64 electron) structure should be disfavored because the first antibonding b_u molecular orbital is at a higher energy than that of the Fe analogue. The fact that 64-electron **7** can be synthesized is, thus, somewhat unexpected. However, the structural data for **7** show that the Ru_4P_2 framework is significantly distorted from the pseudo-octahedral arrangement of atoms in **6**. While the average Ru−Ru bond lengths (2.839 Å in **6**; 2.833 Å in **7**) are almost identical, two of the metal-phosphorus bonds in **7** are short (Ru(1)−P(1) 2.273(2) Å; Ru(2)−P(1) 2.278(2) Å) and two much longer (Ru(1a)−P(1) 2.812(2) Å; Ru(2a)−P(1) 2.737(2) Å) than those in **6** (Ru−P(11) average 2.421; Ru−P(21) average 2.478 Å). Thus the extra eighth electron pair in this 64-electron system may occupy a MO which has significant Ru−P antibonding character.

The infrared spectroscopic data for **7** showed no bands in the bridging carbonyl region, as expected from the solid-state structure. Consistent with the symmetry of the molecule, only one set of ^1H signals was observed for the isopropyl groups and a single ^{31}P resonance at δ 444.8 is in a typical region for a phosphinidene ligand in an electron-precise cluster and at much lower field than for 62-electron "unsaturated" phosphinidene complexes, including **6**.

The origins of the ^{31}P chemical shift differences between 62- and 64-electron phosphinidene clusters have been the subject of considerable debate. Higher field (greater shielding at phosphorus) shifts in the unsaturated 62-electron clusters have been attributed to diamagnetic "ring current" effects similar to that in aromatic compounds.[15a] However, the magnitude of the shift differences, which are often of the order of 200 ppm, is much too large to be accounted for by diamagnetic contributions to $\delta(^{31}P)$.[27] Single-crystal and CP-MAS ^{31}P NMR studies of $Ru_4(CO)_{13}(\mu_3\text{-}PPh)$ have established that the most shielded component of the chemical shift tensor, δ_{33}, lies approximately perpendicular to the Ru_4P square face, with the most deshielded component δ_{11} along the direction of the P−C bond. The close relationship of the structure of $[Ru_4(CO)_{12}(\mu_3\text{-}PPh)]^{2-}$ (**5**) to that of $Ru_4(CO)_{13}(\mu_3\text{-}PPh)$ (**2**) coupled with the similar chemical shifts strongly suggests that the magnitudes and orientations of shielding tensor components in these two molecules are closely aligned. On this basis, the low-field ^{31}P shift in **5** can be confidently attributed to δ_{11} and, following EHMO calculations for **2**, to transitions involving the π_y and π_z orbitals on phosphorus.[27] Although the orientations of the chemical shift tensors for **6** and **7** in their molecular frames are not yet known, one possible explanation for the much higher field ^{31}P shifts in **6** is a stronger interaction between the phosphinidene ligands and the metal atoms, resulting in a *larger* gap between the occupied and unoccupied orbitals on phosphorus and, hence, a larger transition energy. The structural data for **6** and **7** tend to confirm this hypothesis since the Ru−P bond lengths in the 64-electron complex **7** are almost 0.1 Å longer on average than in unsaturated **6**.

Acknowledgment. We thank the Natural Sciences and Engineering Research Council of Canada and the National Research Council of Canada for financial support.

Supporting Information Available: Tables of fractional atomic coordinates and isotropic thermal parameters, bond lengths and angles, anisotropic thermal parameters, and hydrogen coordinates for **5**$[CoCp_2]_2$, **6**, and **7** (22 pages). Ordering information is given on any current masthead page. Structure factor tables are available upon request from the authors.

OM970726C

(26) Field, J. S.; Haines, R. J.; Smit, D. N.; Natarajan, K.; Scheidsteger, O.; Huttner, G. *J. Organomet. Chem.* **1982**, *240*, C23.

(27) Eichele, K.; Wasylishen, R. E.; Corrigan, J. F.; Taylor, N. J.; Carty, A. J. *J. Am. Chem. Soc.* **1995**, *117*, 6961.